Study on Obstacle Avoidance Strategy Using Multiple Ultrasonic Sensors for Spherical Underwater Robots

Chunying Li, *Student Member, IEEE*. Shuxiang Guo, *Fellow, IEEE*. Jian Guo.

***Abstract*—During marine missions, Autonomous Underwater Robots (AUVs) are susceptible to external disturbances, such as obstacles, ocean currents, etc., which can easily cause mission failure or disconnection. Therefore, it is an extremely challenging task to ensure that AUVs have autonomous obstacle avoidance in the presence of multiple stationary and moving obstacles. This paper focuses on developing an obstacle avoidance control strategy for the Spherical Underwater Robot (SUR) we designed based on the ultrasonic sensor array, which considers the robot's kinematic and dynamic model, and ultrasonic sensor characteristics, simultaneously. The control law combines the guidance law and Lyapunov theory to realize real-time following and obstacle avoidance. In addition, a series of simulation and real-environment experiments are performed to validate the proposed control strategy for detecting unknown environments. Furthermore, some comparative experiments are performed and discussed to evaluate the overall performance of the control strategy in terms of the obstacle velocity, total time and tracking error, etc. The experimental results demonstrate the effectiveness and practicability of the proposed control strategy in underwater environment.**

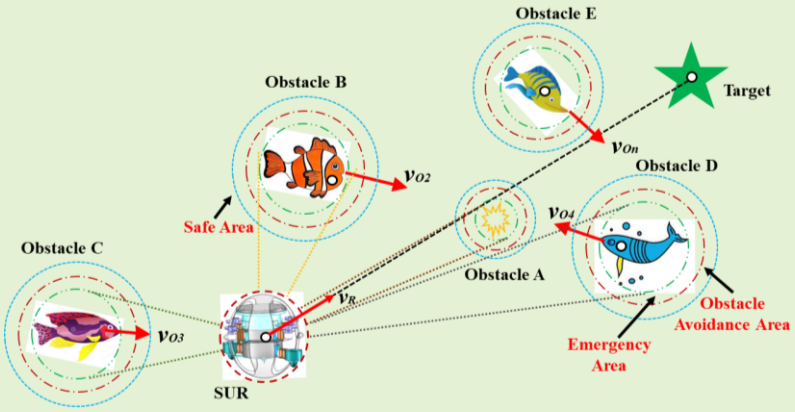

***Index Terms*—Control strategy, obstacle avoidance, ultrasonic sensor array, Spherical Underwater Robot (SUR), kinematic and dynamic analysis, Lyapunov theory**

I. Introduction

Currently AUVs are widely used in marine development, underwater exploration, and military [1]-[3], etc. Considering the complexity and variability of the underwater environment, it is urgent to ensure the safety of AUVs. Especially the autonomous obstacle avoidance capability, which provides a guarantee for AUV to perceive the surrounding environment and respond accordingly [4]-[7].

There are many kinds of sensing devices for AUVs, such as sonar [8], camera [9], ultrasonic sensor [10], and so on. For sonar [8], [11], a device for detecting underwater obstacles and targets, is widely used in large robots such as ships due to its wide scanning coverage. However, it is rarely used on miniature underwater robots considering their size. For the camera [9], [12], considering the specificity and complexity of the underwater environment, the collected information is ambiguous, the AUV locomotion is easily disturbed, and the accuracy cannot be satisfied. Thus, in recent years, underwater ultrasonic sensors [10], [13]-[14], have been widely used in miniature underwater robots to perform various tasks due to their small size, high precision, and strong practicability.

In addition, some obstacle avoidance methods, such as dynamic window, potential field, fuzzy control, and behavior method are the most common. In [15], *Yao et al.* developed an improved Genetic Algorithm (GA) for AUV's path planning in 3D. The simulation verified the effectiveness of the proposed method by considering ocean current. However, this method is challenging to apply in a real environment due to its time-consuming and poor search capability. *Yan et al.* [16]-[17] proposed an adaptive Sliding Mode Control (SMC) for underactuated AUVs with uncertain dynamics and unknown

This work is supported in part by the National Natural Science Foundation of China (61703305), in part by the National High Tech. Research and Development Program of China (No.2015AA043202), in part by the SPS KAKENHI (15K2120), and in part by the China Scholarship Council (CSC) for his doctoral research at Kagawa University under Grant 202208050040.

Corresponding authors: *Shuxiang Guo and Jian Guo*.

C. Li is with the Graduate School of Engineering, Kagawa University, Takamatsu 761-0396, Japan. (e-mail: s21d503@kagawa-u.ac.jp).

S. Guo is with the Key Laboratory of Convergence Medical Engineering System and Healthcare Technology, Ministry of Industry and Information Technology, Beijing Institute of Technology, Beijing 100081, China, and also with the Department of Intelligent Mechanical Systems Engineering, Kagawa University, Takamatsu 761-0396, Japan (e-mail: guo.shuxiang@kagawa-u.ac.jp).

J. Guo is with the Tianjin Key Laboratory for Control Theory and Application in Complicated Systems and Intelligent Robot Laboratory, Tianjin University of Technology, Tianjin, China. (e-mail: jianguo@tjut.edu.cn).

environmental disturbances. *Wang et al.* [18] presented a nonlinear robust controller based on the AUVs' dynamic and command filtered backstepping method. The simulation verified the robustness of the proposed controller. *Fossen et al.* [19] proposed a Line-of-Sight (LoS) guidance law for the path following task considering the kinematic model of AUVs. Although the above three studies provided the solution for tracking problems, they often raise the complexity of the controller, and the obstacle avoidance problem is not addressed which makes them restricted to apply in practice.

When AUV navigates in the underwater environment, it is necessary to avoid obstacles in real-time and ensure its safety, which has also been mentioned in [20]-[23]. However, during the process of AUV obstacle avoidance, it encounters not only stationary obstacles, but also moving obstacles. At the same time, the obstacles not only in front of the robot, but also behind or on the sides, etc. If only a single sensor is used in front of the robot body, it may only detect the obstacles ahead in real-time, but it cannot avoid obstacles in other directions in time. Considering the safety of AUVs in avoiding obstacles, it is necessary to design a multi-sensor array and effective control strategies.

In our previous research, the SUR that uses water-jet and propellers to achieve underwater multi-Degree-of-Freedom (DoF) movements is designed [24]-[26]. The locomotion parameters are obtained and evaluated using fluid dynamic mechanics [27]-[28]. The communication function is evaluated in [29]. Moreover, the path planning and control systems for SUR are conducted in [4], [10], [12]-[13], [30]. In path tracking of SUR, however, the phenomenon that the SUR cannot perceive the surrounding environment in real-time will lead to path following unsuccessfully. It is worth noting that, compared with [4], from the perspective of the particularity of the underwater environment, we found that previous research on target tracking and obstacle avoidance using the optical camera can easily cause the collected sensor information to be ambiguous, and the robot locomotion is easily disturbed. Besides, we have also mentioned in the future work of [4], the importance of SURs' comprehensive perception of the underwater surroundings, which is crucial in practical applications. Secondly, in [10], we aim to complete the detection of underwater information using multi-sensor devices without considering the kinematic and dynamic models of the SUR, which is also one of the performance indicators in this paper. Finally, this paper optimizes the control strategy for the proposed sensor array to improve the obstacle avoidance and tracking performance of SUR by coordinating the information collected by the multi-sensor array.

Based on the above analysis, we designed the sensor array based on the ultrasonic module to improve the obstacle avoidance capability and guarantee the safety of SUR in path tracking. Meanwhile, most researchers focus on prototyping design and path-following control methods [31]. The sensor array is inspired by such excellent performances of the Lateral Line System (LLS) in fish [32]-[33]. Based on the characteristics, AUVs imitate various behaviors of underwater creatures, such as rheotaxis, obstacle avoidance, prey-localization, etc. Few studies are studied in underwater environments for path tracking. Based on our previous research, it is necessary to realize AUVs' trajectory tracking through a sensor array to ensure the robot's safety.

Motivated by the above considerations, in this paper, to perceive the surrounding environment more comprehensively and improve the obstacle avoidance capability in the practical environment, an obstacle avoidance strategy based on multiple ultrasonic sensors is proposed for the SUR. The main contributions of this paper are as follows:

1) From the mentioned literature, it can be seen that developing a general controller that can simultaneously satisfy all the objective items such as stability, nonlinearity, omnidirectional perception capability, obstacle avoidance ability, and robustness is lacking so far. Thus, in order to cover the above deficiencies, a stable, nonlinear controller considering the kinematic and dynamic of SUR is developed, which has a certain reference value for obstacle avoidance and autonomous locomotion capability.
2) According to the particularity of the underwater environment, it is necessary for implementing the omnidirectional perception for AUV. In this paper, the sensor array is designed that are more adaptive and practical for improving tracking and avoiding obstacles. The proposed control strategy is experimentally verified from multiple perspectives, such as moving obstacle velocity, sensor array performance, static and moving obstacles, and has a certain reference value for autonomous obstacle avoidance, especially local obstacle avoidance, for AUVs.
3) Compared to the traditional method, the robot's performance is simulated realistically using Webots, such as path-following and obstacle avoidance in the underwater environment. Furthermore, the robustness, feasibility, and effectiveness of the novel control strategy are verified via some simulations and experiments (including comparative experiments) in the real environment.

The remainder of this paper is organized as follows: Firstly, the kinematic and dynamic model of SUR and the sensor array using multiple ultrasonic sensors is described in Section II. Then, the control strategy for SUR is developed in Section III. Afterward, Section IV uses the Webots simulation to validate the performance of the proposed control strategy considering the dynamic model of SUR. A series of experiments in the real environment is also carried out to verify the effectiveness of the proposed control scheme in Section V. Then, some comparative experiments are analysed and discussed in Section VI. Finally, Section VII concludes the paper.

II. Multiple Ultrasonic Sensors for SUR

In this section, kinematic and dynamic models of the SUR is represented, and the sensor array is designed based on the SUR's mathematical model.

A. Kinematic and Dynamic Models

Fig. 1 is the coordinate frames of the SUR-fixed {B} and the Earth-fixed {E}. The SUR has four DoFs $[x, y, z, \psi]^T$, including surge, sway, heave, and yaw [28], which are considered to achieve obstacle avoidance. The motion of the SUR in four DoFs can be described as follows:

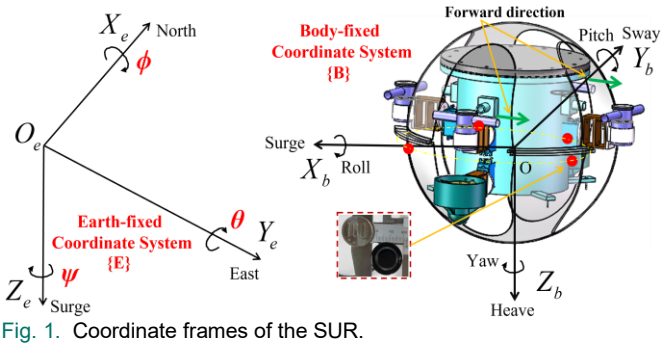

Fig. 1. Coordinate frames of the SUR.

$$\boldsymbol{\eta} = [x, y, z, \psi]^T$$
$$\boldsymbol{v} = [u, v, w, r]^T \quad (1)$$

where $\boldsymbol{\eta}$ represents the position and orientation vector of SUR in {E} system. x, y, z are the coordinates of position and ψ is orientation coordinates along Z_e axes. $\boldsymbol{v}$ is the velocity and angular velocity in {B} system. u, v, w linear velocities and r is the angular velocity of the turning.

The corresponding Jacobian matrix $\boldsymbol{J(\eta)}$ can be expressed as:

$$\begin{Bmatrix} \dot{x} \\ \dot{y} \\ \dot{z} \\ \dot{\psi} \end{Bmatrix} = \begin{bmatrix} c\psi & -s\psi & 0 & 0 \\ s\psi & c\psi & 0 & 0 \\ 0 & 0 & 1 & 0 \\ 0 & 0 & 0 & 1 \end{bmatrix} \begin{Bmatrix} u \\ v \\ w \\ r \end{Bmatrix} = \boldsymbol{J(\eta)} \begin{Bmatrix} u \\ v \\ w \\ r \end{Bmatrix} \quad (2)$$

where s and c are the abbreviations of sin and cos, respectively.

The dynamic model of SUR can be extracted using the Lagrange method, and can be rewritten as:

$$\begin{cases} \dot{u} = \dfrac{m_{22}}{m_{11}} vr - \dfrac{X_u}{m_{11}} u - \dfrac{X_{u|u|} u|u|}{m_{11}} + \dfrac{F_u}{m_{11}} \\ \dot{v} = -\dfrac{m_{11}}{m_{22}} ur - \dfrac{Y_v}{m_{22}} v - \dfrac{Y_{v|v|} v|v|}{m_{22}} + \dfrac{F_v}{m_{22}} \\ \dot{w} = -\dfrac{Z_{w|w|} w|w|}{m_{33}} + \dfrac{F_w}{m_{33}} \\ \dot{r} = \dfrac{m_{11} - m_{22}}{m_{44}} uv - \dfrac{N_r r}{m_{44}} - \dfrac{N_{r|r|} r|r|}{m_{44}} + \dfrac{F_r}{m_{44}} \end{cases} \quad (3)$$

where F_u = force applied to the X_b-axis of the body for linear motion, F_v = force applied to the Y_b-axis of body for linear motion, F_w = force applied to the Z_b-axis of body for linear motion, F_r = force applied to the body for angular motion; m_{11}, m_{22} and m_{33} represent the combined rigid body and added mass terms; And m_{44} represents the combined rigid body and added moment about Z_b-axis. X_u, Y_v, N_r are the linear and quadratic terms coefficients, and $X_{u|u|}, Y_{v|v|}, Z_{w|w|}, N_{r|r|}$ are the nonlinear drag coefficients [4], [23], [34]-[36].

B. Ultrasonic Sensor Array

In the unknown and complex underwater environment, the SUR perceives the external environment through sensors fixed in the body to perform tasks. Among various sensor detection methods, the ultrasonic sensor system is widely used because of its low-cost, easy-installation, and not easy to be disturbed by electromagnetic and light. Thus, in this paper, the underwater ultrasonic module (JSN-SR0T4) is used for detecting the underwater environment. The ultrasonic module has the characteristics, such as small-size, convenience, low-power-consumption, high-accuracy, small-blind-area, and high-resolution. Its specific parameters are shown in Table I.

TABLE I
FEATURES OF THE ULTRASONIC SENSOR JSN-SR0T4

Items	Characteristics	Items	Characteristics
Size	41 x 28.5 x 12 mm	Environment	Air or Water
Supply Voltage	DC 5V	Probe Frequency	40 KHZ
Distance	Min: 0.2 m; Max: 4.5 m	Resolution	About 5 mm

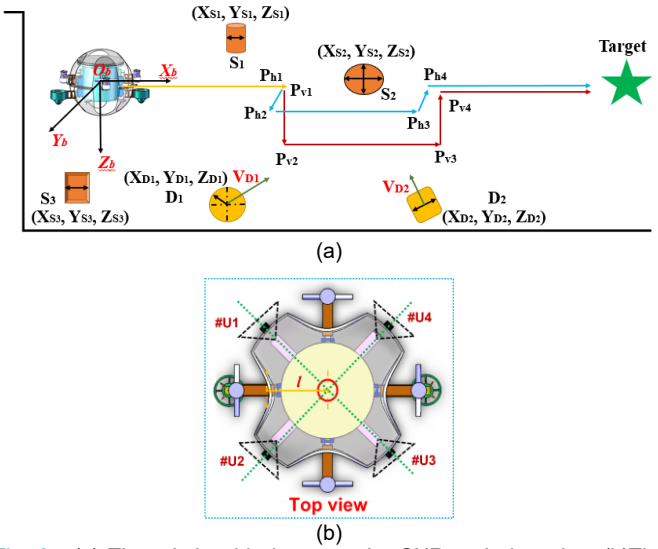

Fig. 2. (a) The relationship between the SUR and obstacles; (b)The sensor array designed for SUR using ultrasonic modules.

As the eyes of the SUR, the sensor array can provide real-time sensing information in an unknown environment to execute tasks safely and improve the efficiency of the SUR. SUR surpasses obstacles by changing the depth and or moving horizontally, as shown in Fig. 2 (a), where S and D represent static and moving obstacles, respectively. In order for SUR to fully perceive the surrounding environment and avoid obstacles, based on the mathematical model and fluid mechanics of SUR, the sensor array using ultrasonic sensors is designed, as shown in Fig. 2 (b). A total of four ultrasonic sensors are used. Symmetrically distributed around the robot body. The specific obstacle avoidance strategy will be described in Section III.

The acquisition time of the whole ultrasonic detecting system is set as follows: when the robot moves, the detecting system is triggered, and the information is collected cyclically from #U1 to #U4. $T = 4 \times \Delta T$, where ΔT is the time delay of a single ultrasonic sensor. The cycle time is set to be less than 0.1 s in this paper. Each A/D port is collected 5 times in each sampling sequence. Noted that the A/D conversion time is less than 0.005s, and the conversion precision is 8-bit. Thus, the total ranging error can be calculated, which is less than 0.02 m.

TABLE II
TEST RESULTS OF THE ULTRASONIC SENSOR (#U1)

D_A/cm	D_M/cm		Error/%		D_A/cm	D_M/cm		Error/%		D_A/cm	D_M/cm		Error/%	
	Air	*Water*	*Air*	*Water*		*Air*	*Water*	*Air*	*Water*		*Air*	*Water*	*Air*	*Water*
25	25	26	0.0	4.0	85	83	82	2.4	3.6	145	147	148	1.4	2.1
35	36	34	2.9	2.9	95	96	93	1.1	2.1	155	156	156	0.6	0.6
45	46	47	2.2	4.4	105	103	106	1.9	1.0	165	164	165	0.6	0.0
55	55	54	0.0	1.8	115	114	115	0.9	0.0	175	177	176	1.1	0.6
65	66	65	1.5	0.0	125	125	124	0.0	0.8	185	186	187	0.5	1.1
75	74	73	1.3	2.7	135	136	137	0.7	1.5	195	195	194	0.0	0.5

The maximum velocity of SUR is less than 0.25 m/s, which is mentioned in [24]-[26], [37]-[38], so it can meet the needs of underwater detection.

The progressive standard deviation $S^2(i)$ of sampled data $d_a(i),(1 \le i \le n)$ at time *t* is defined as follows:

$$S^2(i) = \overline{d_a^2(i)} - (\overline{d_a}(i))^2 \tag{4}$$

where *n* is the length of the sampled data, $\overline{d_a^2(i)}$ is the value that is squared first and then smoothed. $(\overline{d_a}(i))^2$ is the value that is smoothed first and then squared.

The new data $d_a(i+1)$ at time $t+1$ satisfies:

$$\overline{d_a}(i) - \lambda_1 S(i) < d_a(i+1) < \overline{d_a}(i) + \lambda_1 S(i) \tag{5}$$

where λ_1 is a positive real number. If λ_1 is zero, $d_a(i+1) = \overline{d_a}(i)$.

C. Adaptive Model for Ultrasonic Sensors

In the multi-ultrasonic detecting system, to reduce the error caused by noise, the weighted average method is used to preprocess the collected data. In addition, to avoid glitch phenomenon in data acquisition, adaptive filtering is used, as shown in Algorithm 1.

In order to improve the sensitivity and robustness of the ultrasonic sensor for environmental detection, in the obstacle avoidance strategy, we perform effective avoidance according to the distance between the SUR and the obstacle, and use weighting factors in different distance ranges to constrain. To further improve the noise immunity of the ultrasonic sensor, we use the historical memory item method, namely:

$$\theta_{n+1} = \theta_n + 2\mu\Re_n X_n + \beta_n(\theta_n - \theta_{n-1}) \tag{6}$$

where β_k is the historical memory factor, which depends on the corrected error e_n. The corrected error e_n of the current frame and variance of the corrected error σ_n^2 satisfy:

$$\begin{aligned} e_n &= \frac{1}{N}\sum_{i=1}^{n} |e_i| w_i \\ \sigma_n^2 &= \frac{1}{N-1}\sum_{i=1}^{n} (|e_i| w_i - e_n)^2 \end{aligned} \tag{7}$$

When the corrected error of the *n-th* time is smaller than the historical statistical error, it means that the current weight coefficient vector does not need to be corrected; Otherwise, the weight coefficient vector needs to be corrected.

Algorithm 1: Adaptive Least Squares Estimation.

S1: Define the current input data sequence X_n and weight coefficient vector $\boldsymbol{\theta_k}$, which is obtained by the least squares method as:

$$X_n = [x_{n-1}, x_n, \cdots, x_{n-m}]^T;\ \theta_n = [\theta_{1n}, \theta_{2n}, \cdots, \theta_{kn}]$$

S2: Thus, the weighted sum of data can be expressed as:

$$Y_n = \theta_{1n}x_{n-1} + \theta_{2n}x_n + \cdots + \theta_{kn}x_{n-m}$$

S3: The residual can be expressed using the least squares fit as:

$$\Re_n = X_n - Y_n = X_n - (\theta_{1n}x_{n-1} + \cdots + \theta_{kn}x_{n-m})$$

The input data sequence at time $n+1$ is:

$$X_{n+1} = [x_n, x_{n-1}, \cdots, x_{n-m+1}]^T;\ \theta_{n+1} = \theta_n - \mu\nabla(\Re)$$

where the estimated gradient $\nabla(\Re)$ can be solved by the gradient of a single error squared sample, satisfying:

$$\nabla(\Re_n) = 2\Re_n \nabla[x_n - \theta_n^T X_n] = 2\Re_n X_n$$

S4: Thus, the adaptive estimation algorithm can be expressed as:

$$\theta_{n+1} = \theta_n + 2\mu\Re_n X_n$$

where μ is the step factor, which can be constrained by the autocorrelation matrix $\boldsymbol{R}$, satisfying:

$$0 < \mu < \frac{1}{trR}, R = [x_n^{'}][X_n^{'}]^T$$

S5: In this paper, the optimal step factor can be expressed as:

$$\mu_n = \frac{g_n^T g_n}{g_n^T R_n g_n}$$

where $g_n = X_n\Re_n$.

Then, to test the performance of ultrasonic sensors in detail and comprehensively, the distance measurement experiment is performed in air and water, and the absolute error is calculated. Take the #U1 as an example for testing. Test results are shown in Table II, D_A and D_M represent the desired and measured distance, respectively. It can be seen that the absolute error of the measurement distance is less than 4.5 cm. Especially at distances greater than 25 cm, its performance is better, which can meet the needs of underwater environment detection.

III. THE PROPOSED CONTROL STRATEGY FOR SUR

Assumed that the underwater robot will encounter different obstacles, including static or moving obstacles in underwater environment. In this section, the tracking and obstacle avoidance strategy is proposed to guide the SUR to complete the mission. The control method based on Lyapunov is developed which is robust against external disturbances and autonomous avoiding obstacles associated with behavior and

parametric uncertainties of the system. Thus, obstacle avoidance strategies considering sensor array and avoidance obstacle behavior is a necessary task.

A. Trajectory Tracking

In this section, the SUR is supposed to track the desired trajectory and its workspace states should follow the reference path in a stable robust way. We define the tracking error of the SUR as follows:

$$\begin{cases} x_e = (x - x_d)\cos\gamma_d + (y - y_d)\sin\gamma_d \\ y_e = -(x - x_d)\sin\gamma_d + (y - y_d)\cos\gamma_d \\ z_e = z - z_d \end{cases} \tag{8}$$

where $\gamma_d = a\tan 2(\dot{y}_d, \dot{x}_d)$. The derivation of x_e, y_e and z_e satisfies, detail in [5]:

$$\begin{aligned} \dot{x}_e &= \sqrt{(U_v\cos\alpha)^2 + v^2}\cos(\psi - \gamma_d) \\ &\quad -\sqrt{(\dot{x}_d)^2 + (\dot{y}_d)^2} + y_e\dot{\gamma}_d \\ \dot{y}_e &= \sqrt{(U_v\cos\alpha)^2 + v^2}\sin(\psi - \gamma_d) - x_e\dot{\gamma}_d \\ \dot{z}_e &= U_v\sin\alpha - \dot{z}_d \end{aligned} \tag{9}$$

where $U_v = \sqrt{u^2 + w^2}$, $\alpha = a\tan 2(w, u)$.

Define *T(t)* as the following path, where *t* is the time. The current position and target position satisfy that:

$$\begin{aligned} T(t_0 + t) &= x(t_0 + t) + y(t_0 + t) \\ T(t) - e_1 &\le y, z \le T(t) + e_1 \end{aligned} \tag{10}$$

where e_1 is the maximum tracking error, satisfies $e_1 = \xi - \xi_{e1}$.

Then, the Lyapunov function is used to prove the stability of SUR, as follows:

$$V_1 = \frac{1}{2}\|e_1\|^2 = \frac{1}{2}(x_e^2 + y_e^2 + z_e^2) \tag{11}$$

The time derivation of V_1 yields:

$$\begin{aligned} \dot{V}_1 &= (-k_1 x_e + y_e\dot{\gamma}_d)x_e + (-\sqrt{(U_v\cos\alpha)^2 + v^2} \\ &\quad -x_e\dot{\gamma}_d)y_e + (-k_2 z_e)z_e \\ &= -k_1 x_e^2 - \frac{\sqrt{(U_v\cos\alpha)^2 + v^2}}{\sqrt{y_e^2 + \Delta_h^2}}y_e^2 - k_2 z_e^2 \\ &= -[x_e \;\; y_e \;\; z_e]\begin{bmatrix} k_1 & 0 & 0 \\ 0 & \dfrac{\sqrt{(U_v\cos\alpha)^2 + v^2}}{\sqrt{y_e^2 + \Delta_h^2}} & 0 \\ 0 & 0 & k_2 \end{bmatrix} := M\begin{bmatrix} x_e \\ y_e \\ z_e \end{bmatrix} \\ &= -e_1^T M e_1 \le \|e_1\|^2\|M\| \le 0 \end{aligned} \tag{12}$$

Noted that the designed control gains k_1, $k_2 > 0$, thus $\boldsymbol{M}$ is a positive definite matrix.

B. Priority Assignment Model for Sensor Array

The multi-sensor array decomposes the information detected in multiple directions. Each sensor controls a sub-task independently, which is determined by the sub-task function. Then, each sub-task has a different priority. So the comprehensive output function can be obtained by the Null-Space-Behavior (NSB) method, which can be passed to the SUR's actuator to control the behavior.

Define the task variable as P, satisfies $P = f(\eta)$. The derivation of P yields:

$$P' = \frac{\partial f(\eta)}{\partial \eta} = \boldsymbol{J(\eta)}v \tag{13}$$

The least squares solution of the velocity matrix $\boldsymbol{v_d}$ yields:

$$v_d = J^T(JJ^T)^{-1}(P_t' + \kappa\tilde{P}) \tag{14}$$

where P_t' is the desired value of the task variable, $\tilde{P} = P_t - P$, and $\boldsymbol{\kappa} > 0$ is a positive gain matrix.

Let *i* be the priority of tasks, when $i = 1$, indicates the highest priority. The velocity of the *i-th* task satisfies:

$$v_{i,d} = J_i^T(J_iJ_i^T)^{-1}(P_{i,t}' + \kappa\tilde{P}_i) \tag{15}$$

By spatially projecting low-level task to high-level task, the velocity of the overall control objective ($i = 4$) can be expressed as:

$$v_d = v_1 + N_1(v_2 + N_2(v_3 + N_3v_4)) \tag{16}$$

where N_i represents the spatial projection of *i - 1* to *i*.

C. Proposed Control Scheme

As shown in Fig. 3 (a), the relationship between the current position of the SUR and obstacle is constructed. The kinematic equation of the obstacle satisfies:

$$\begin{cases} \dot{x}_{OB} = u_{OB}\cos\psi_{OB} \\ \dot{y}_{OB} = -u_{OB}\sin\psi_{OB} \end{cases} \tag{17}$$

where $[x_{OB} \;\; y_{OB} \;\; \psi_{OB}]^T$ represents the position and attitude, and u_{OB} is the velocity of the moving obstacle, which is measured in a real environment with an observation system (base station-based), described in Section V.

Fig. 3 (b) shows the situation when the moving obstacle is considered, ψ_R^B is the motion direction of the SUR relative to the obstacle in the body coordinate system, and the range is -180° to 180° (the conventional four-quadrant is defined as 0° to 360°). So if $\psi_R^B < 0$, add 360° to meet the requirements. When ψ_R^B is in the first and second quadrants, the clockwise direction is selected; Otherwise, the counterclockwise direction is selected, so as to ensure the safety of the path.

When encountering moving obstacles, The distance *l*

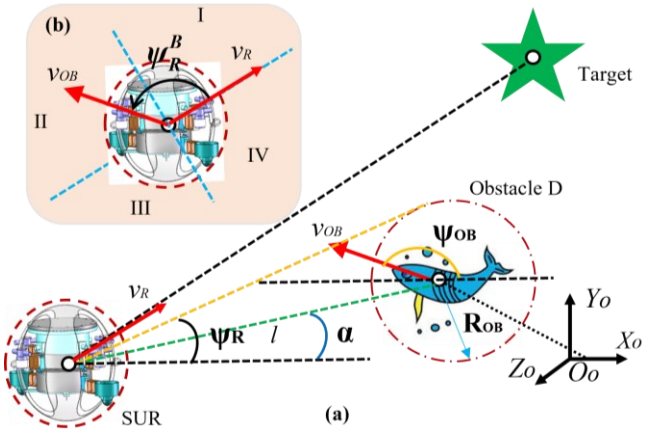

Fig. 3. The principle for the obstacle avoidance of SUR.

between the SUR and the moving obstacle yields:

$$l=\sqrt{(x_{OB}-x_R)^2+(y_{OB}-y_R)^2} \tag{18}$$

Importantly, when encountering the moving obstacle, the avoidance velocity u_{dm}, which is a variable, must be greater than the velocity v_{OB} of the moving obstacle. The magnitude v_{dm} and direction angle ψ_{dm} of the avoidance velocity vector u_{dm} are defined as:

$$\begin{cases} v_{dm}\in[v_{dm\_\min},v_{dm\_\max}] \\ \psi_{dm}\in[\psi_{dm\_\min},\psi_{dm\_\max}] \end{cases} \tag{19}$$

where $v_{dm\_\min}=v_{dm}-\gamma_0, v_{dm\_\max}=v_{dm}+\gamma_0$, $\gamma_0=at$, $\psi_{dm\_\min}=\psi_{dm}-\sigma_0, \psi_{dm\_\max}=\psi_{dm}+\sigma_0, \sigma_0=\sqrt{a/R_{OB}}\,t$. a and t are the acceleration and obstacle avoidance time of the SUR, respectively.

The updated angle ψ_{dm} of the SUR yields:

$$\psi_{dm}=\varphi+\lambda_2\left(\frac{\pi}{2}-\arctan\frac{l_{dm}+\delta}{k_3R_{OB}}\right) \tag{20}$$

where φ represents the angle of the obstacle position relative the SUR position, $l_{dm}=l-R_{OB}$ represents the shortest distance between the SUR and the obstacle, the variable δ is used to ensure the safety of SUR, and k_3 is the convergence coefficient to ensure SUR convergence to the anti-collision space. Noted that the value λ_2 depends on φ, if the position range belongs to [-180°, 0°], the $\lambda_2=-1$. Conversely, $\lambda_2=1$, when the position range belongs to [0°, 180°].

D. Stability Analysis

Based on the above analysis, in order to verify the stability of obstacle avoidance of the SUR, the Lyapunov function $V_2=\frac{1}{2}e_2^2$ is chosen, Time derivation of V_2 is.

$$\dot{V}_2=e_2\dot{e}_2=e_2(\dot{l}-\dot{R}_{OB}) \tag{21}$$

Based on the definition φ, the relationship between l and φ can be expressed as:

$$\begin{cases} l\cos\varphi=x_O-x_d \\ -l\sin\varphi=y_O-y_d \end{cases} \tag{22}$$

Substituting (20) and (22) into (21) yields:

$$\begin{aligned} \dot{V}_2&=e_2\left(\left(l\cos\varphi(\dot{x}_O-\dot{x}_d)-l\sin\varphi(\dot{y}_O-\dot{y}_d)\right)/l\right) \\ &=e_2[\cos\varphi(u_{OB}\cos\psi_{OB}-u_d\cos\psi_d) \\ &\quad-\sin\varphi(-u_{OB}\sin\psi_{OB}+u_d\sin\psi_d)] \\ &=e_2[u_{OB}\cos(\varphi-\psi_{OB})-u_d\cos(\psi_d-\varphi)] \end{aligned} \tag{23}$$

With (20), (23) can be written as:

$$\begin{aligned} \dot{V}_2&=e_2[-u_{dm}\cos(\frac{\pi}{2}-\arctan\frac{l_{dm}+\delta}{k_3R_{OB}}) \\ &\quad-u_{OB}\cos(\pi-\varphi+\psi_{OB})] \\ &\le\frac{-u_{dm}e_2^2}{\sqrt{k_3^2R_{OB}^2+(l_{dm}+\delta)^2}}=\frac{-2u_{dm}}{\sqrt{k_3^2R_{OB}^2+(l_{dm}+\delta)^2}}V_2 \end{aligned} \tag{24}$$

Considering $t\to\infty$, V_2 approaches 0. Thus, V_2 is asymptotically stable. And the proposed control strategy can ensure that the SUR avoids obstacles effectively.

IV. Simulation Results

To verify the effectiveness and stability of the proposed control strategy for the sensor array of SUR, a series of simulation experiments (two scenarios) are considered in Webots. In the first scenario, four stationary obstacles are located in the reference path. In the second scenario, two moving obstacles and one stationary obstacle are located in the reference path. All experiments are performed in the water tank.

A. Software Setup

Webots is a physical simulation software that can realistically simulate the autonomous motion of underwater robots using the ODE engine. The SUR model we built was imported into a water tank with a length x width x height of 10 m × 5 m × 5 m. The underwater environment settings are shown in Fig. 4. After importing the model, we added the sensor array,

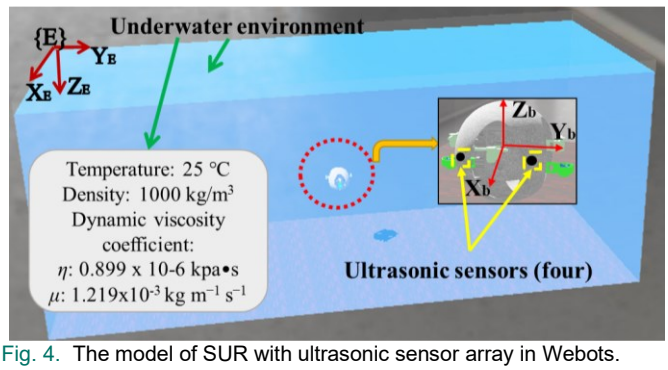

Fig. 4. The model of SUR with ultrasonic sensor array in Webots.

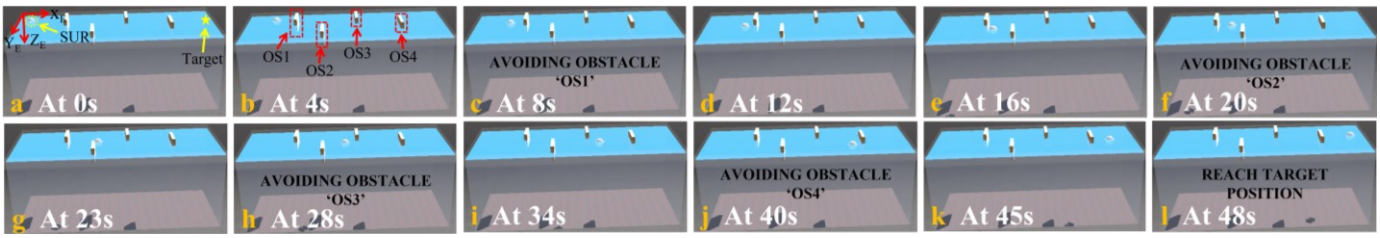

Fig. 5. Following process of SUR in presence of the static obstacles (in simulation).

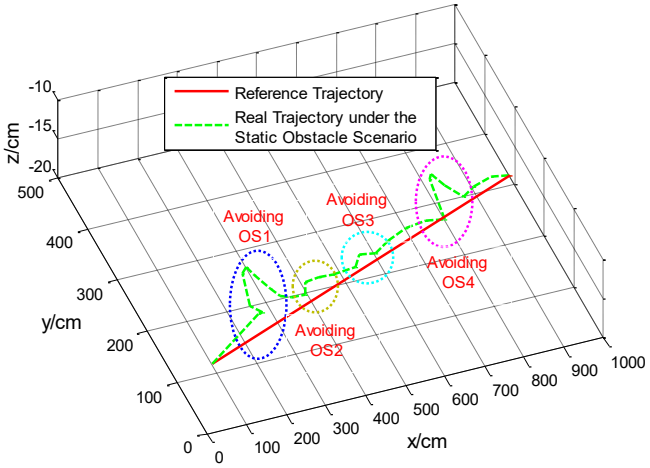

Fig. 6. Trajectory tracking result of SUR in presence of the static obstacles (in simulation).

a total of four ultrasonic sensor nodes were added, and its node properties were set. Noted that sensors need to be configured according to the importing robot model, marked as Fig. 4. The communication protocol adopts TCP/IP wireless communication, which is consistent with the communication device used in experiments. Next, to verify the performance of the sensor array designed, a series of experiments in Webots were performed.

B. First Scenario Study

In the first scenario, to demonstrate the avoidance obstacle capability of proposed control strategy under multiple static obstacles, four stationary obstacles, with 1.6 m × 0.3 m × 0.8 m (length × width × depth), are placed within the desired trajectory in the positions x_{OS1}=*2.5 m*, y_{OS1}= *1.2 m*, x_{OS2}=*4 m*, y_{OS2}=*3.8 m*, x_{OS3}= *6 m*, y_{OS3}=*1.2 m*, x_{OS4}= *8 m*, y_{OS4}= *2.5 m*. The distance of *z*-axis, which refers to the distance from the center of obstacle to the water surface, is -0.15 m.

The obstacle avoidance process of the SUR is shown in Fig. 5. The SUR starts from the starting position, see Fig. 5 (a). Then, the robot bypasses obstacles *OS1*, *OS2*, *OS3*, *OS4* in turn. After avoiding obstacles, the SUR will move towards the target. The target position is x_{Target}= *9.5 m*, y_{Target}= *2.5 m*. It can be seen that the SUR can pass obstacles successfully.

Here it also can be seen from Fig. 6 that the SUR can convergence to the tracking trajectory, the trajectory is smooth, and the robot can pass obstacle successfully, which demonstrates the effectiveness and stability of the proposed control strategy.

C. Second Scenario Study

In this section, the obstacle avoidance experiment of SUR under the static and moving obstacles are performed. In the unknown and complex underwater environment, there may be obstacles form all directions. The multi-sensor array acts as the eyes of the SUR, sensing the surrounding environment in real time to safely perform tasks. The multi-sensors cooperate to improve the perception capability of the surrounding environment and the execution efficiency of SUR.

Thus, to validate obstacle avoidance capability of the sensor array we designed for SUR, one static obstacle, *OS1*, two moving obstacles, *OM1* and *OM2*, are placed within the desired trajectory in the positions x_{OS1}=*8.0 m*, y_{OS1}= *1.2 m*, x_{OM1}=*0.5 m*, y_{OM1}= *4.5 m*, x_{OM2}=*4.5 m*, y_{OM2}=*1.5 m*. Noted that the moving obstacles are the same size as the SUR. The velocity v_{OM1} of the moving obstacle is greater than the velocity v_{SUR} of the SUR to ensure that the SUR encounters the obstacle *OM1*. The moving obstacles (*OM1* and *OM2*) follow the path, and the target positions of the OM1 and OM2 are set to T_{OM1} *(4.5m, 2.5 m)*, T_{OM2} *(7.5 m, 2.0 m)*, respectively. The center position of the static obstacle *OS1* is on the reference path.

The locomotion process under static and moving obstacles is shown in Fig. 7. From Fig. 7 (a) - (b), the SUR follows the reference path. When detecting a moving obstacle behind, from Fig. 7 (c) - (f), the obstacle avoidance mode is dominant. At 28 s, after avoiding moving obstacles *OM1* and *OM2*, the SUR tracks the path again and the cruise mode is dominant. From Fig. 7 (g), SUR detects the obstacle ahead and continues to avoid the obstacle. After avoiding the obstacle, from Fig. 7 (h) - (j), continue to track the reference path until reaching the target position T_{SUR}.

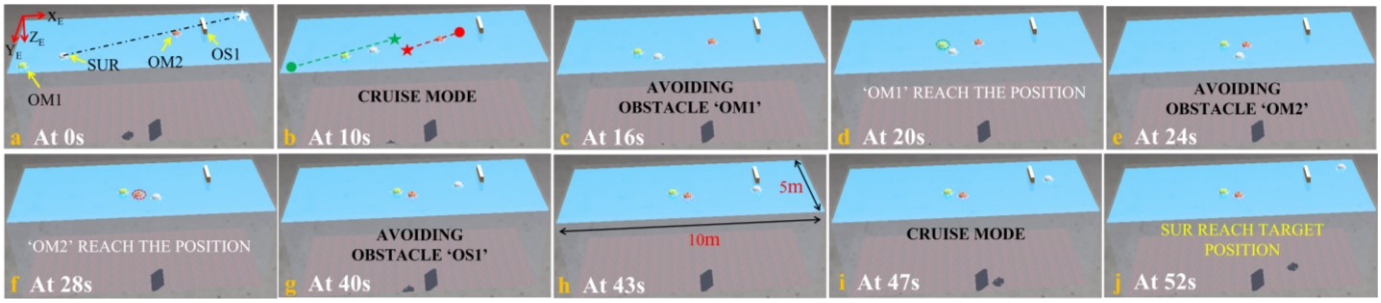

Fig. 7. Following process of SUR in presence of the static and moving obstacles (in simulation).

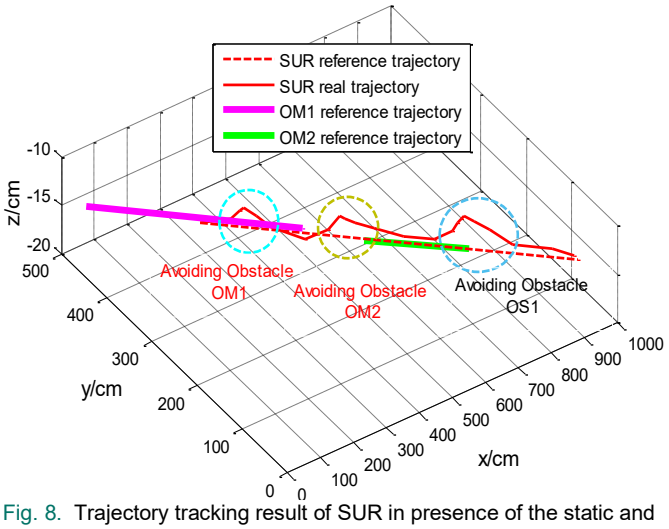

Fig. 8. Trajectory tracking result of SUR in presence of the static and moving obstacles (in simulation).

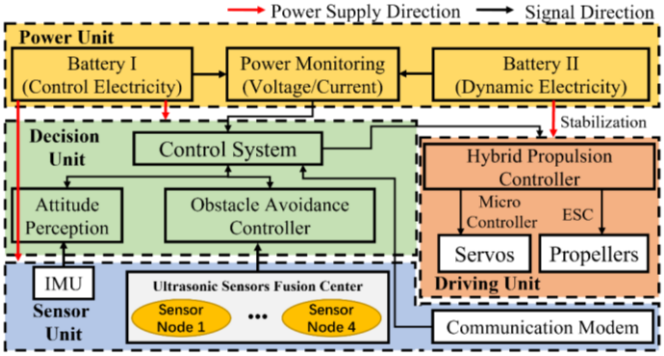

Fig. 9. The block diagram of control system for the SUR using multi ultrasonic sensors.

The trajectory of SUR under static and moving obstacles is shown in Fig. 8. It can be seen that the SUR can safely avoid stationary and moving obstacles, which verifies the effectiveness of the designed sensor array and the practicability and stability of the control strategy.

V. Experimental Results

Some related experiments are also performed to validate the effectiveness and practicability of the proposed control strategy for SUR's sensor array in an experimental pool (length: 3 m, width: 2 m, depth: 1 m).

A. The Control System

The SUR prototype we constructed with diameter of 540 mm is 7.9 Kg in air. To improve the stability and logic of the control system, four parts, including the Power Supply Unit, the Decision Unit, the Sensor Unit, and the Driving Unit, are divided, as shown in Fig. 9. Among them the power monitoring system consists of three detachable batteries, one (Battery I) of which powers the control system and sensor unit, and two (Battery II) of which powers the hybrid drive system. Battery working time is typically about 2 hours during experiments. In the experiments, the high symmetry of the SUR is beneficial for the control of the robot dynamics. In addition, four ultrasonic sensors (see Fig. 1) and communication device (Micron Data Modem (Tritech)) are used to collect information of the surrounding environment and communicate in real time to ensure that the SUR can perform tasks safely. In [39], *Gu et al.* introduced the use of base stations. A nine-axis IMU is utilized and used to perceive and adjust the robot attitude. In this paper, the velocity of the moving obstacle is measured with the observation system, detail in [37], [39]-[40], which consists of a camera and base station. The camera is fixed above the pool, and the base station is used for real-time communication between the robot and the observation system.

Fig. 10. The movement process of the SUR in in presence of the static obstacles (in real environment).

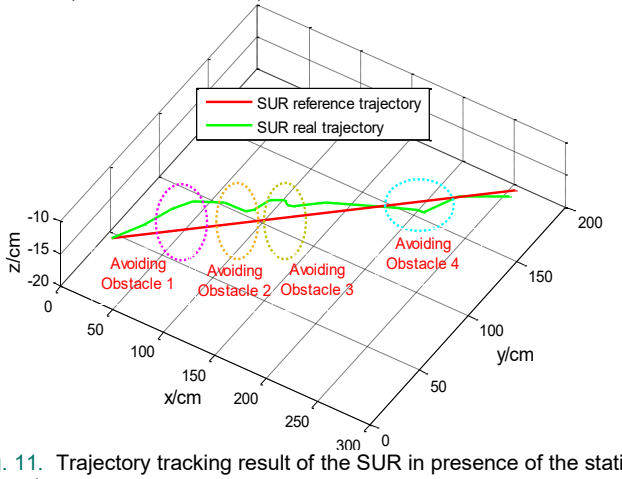

Fig. 11. Trajectory tracking result of the SUR in presence of the static obstacles.

B. Experiments under Static Obstacles

In the first experiment, the SUR performed a cruise mission in the presence of static obstacles, with a depth of $z = -0.15$ *m*. The initial position of SUR is *(0.25 m, 0.25 m)*. Four stationary obstacles with a diameter of 0.1 m were placed at the position are placed in the positions $x_{Obstacle1}$=*0.6 m*, $y_{Obstacle1}$= *0.35 m*, $x_{Obstacle2}$=*1.2 m*, $y_{Obstacle2}$=*0.7 m*, $x_{Obstacle3}$= *1.2 m*, $y_{Obstacle3}$=*1.5 m*, $x_{Obstacle4}$= *2.0 m*, $y_{Obstacle4}$= *1.0 m*.

The movement process of the SUR is shown in Fig. 10. Initially, the SUR starts to move from the initial position, see

Fig. 10 (a1). Then, the robot detected the obstacle (*Obstacle 1*) and avoided it. The mission ended when SUR reached the target position. The target position is x_{Target}= *2.75 m*, y_{Target}= *1.0 m*. It can be seen from Fig. 10 that the SUR can pass obstacles successfully. Noted that, due to the existence of external factors, such as wind, water waves, obstacles will move in a small range, about 0.05 m under static obstacle experiments.

Fig. 11 shows the tracking trajectory of SUR in presence of static obstacles. As can be seen, SUR using the proposed control strategy successfully reaches the target position. It should be remarked that the curves of the experimental data swing in the obstacle avoidance process because the transient shock caused by water waves. Moreover, the robot can rapidly follow the reference path after avoiding obstacles. At about 20 s, SUR reaches the target position.

C. Experiments under Moving Obstacle

In the second experiment, two scenarios with moving obstacles are considered to verify the effectiveness and feasibility of the designed sensor array and proposed control strategy. *Scenario 1*: The SUR moves relative to the moving obstacle (*Moving Obstacle*), see Fig. 12. That is, the moving obstacle is located in front of the SUR. The starting position of the moving obstacle is *(2.75 m, 1.75 m)*, which is consistent with the target position of the SUR. And the target position of the moving obstacle is consistent with the starting position *(0.25 m, 0.25 m)* of the SUR. Noted that the velocity of the SUR and the moving obstacle is the same, $v_{SUR} = v_{Moving\ Obstacle} = 0.2$ *m/s*. *Scenario 2*: The moving obstacle is behind the SUR, see Fig. 14. The velocity $v_{Moving\ Obstacle}$ of the moving obstacle is greater than the velocity v_{SUR} of the SUR, namely, $v_{Moving\ Obstacle}$ = 0.2 m/s, v_{SUR}= 0.15 m/s.

Fig. 12 shows the movement process of the SUR when there is a moving obstacle ahead. Form Fig. 12 (b) - (c), the SUR is avoiding the moving obstacle. After avoiding the obstacle, the SUR tracks the reference trajectory immediately until reaching the target position. The trajectory of the SUR is shown in Fig. 13. It can be seen that the SUR can rapidly avoid obstacles when the robot detects the obstacle at 6 s.

In addition, experiments with the moving obstacle located behind the SUR were performed, as shown in Fig. 14. The initial positions of the SUR and the moving obstacle are *(1.0 m, 0.8 m)* and *(0.25 m, 0.25 m)*, respectively. The target location is the same, which is *(2.75 m, 1.75 m)*. The velocity of moving obstacle $v_{Moving\ Obstacle}$ and SUR v_{SUR}, are 0.2 m/s and 0.15 m/s respectively. Noted that when the moving obstacle reaches the target position, the operator will pick it up so as not to affect the SUR operation.

The tracking trajectory of the SUR is shown in Fig. 15 when there is a moving obstacle behind. From Fig. 13 and Fig. 15, the moving obstacles appear during the time period of about 6 s. As can be seen, the SUR can successfully bypass the mentioned moving obstacles. The proposed control strategy has the related mission with high sensitivity and less deviation respect to the desired trajectory.

VI. Discussion

The proposed control strategy confers advantages for real-time tracking and obstacle avoidance of SUR. Based on the above analysis, SUR can pass the static and moving obstacles successfully. For a comprehensive evaluation of the proposed control strategy, some related comparative experiments are performed.

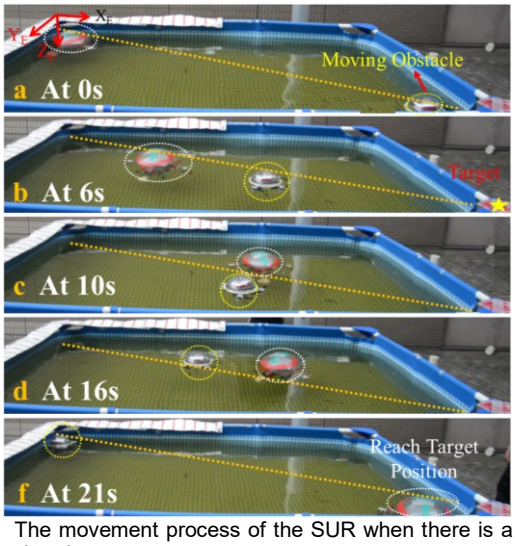

Fig. 12. The movement process of the SUR when there is a moving obstacle ahead.

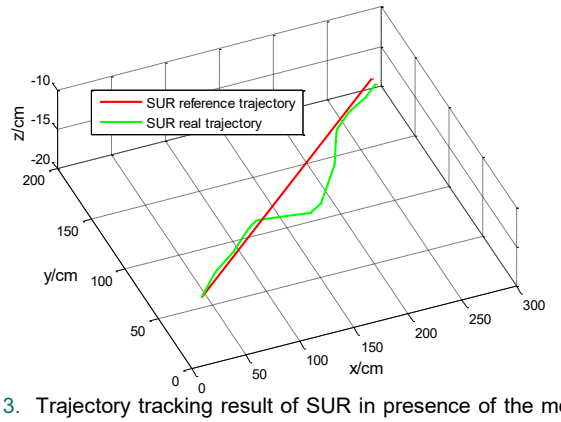

Fig. 13. Trajectory tracking result of SUR in presence of the moving obstacle ahead.

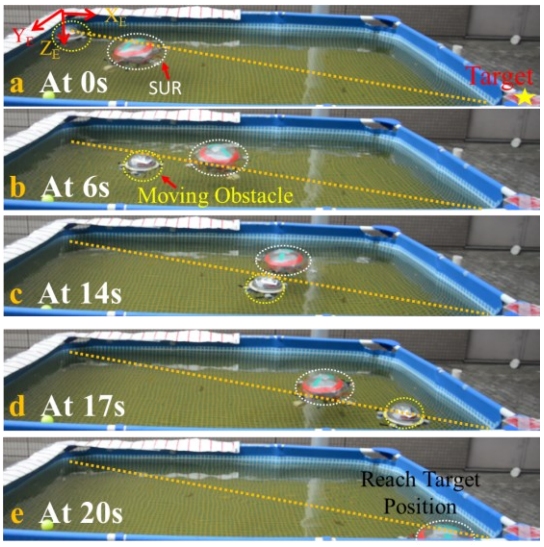

Fig. 14. The movement process of the SUR when there is a moving obstacle behind.

A. Performance of the Control Strategy under Moving Obstacle with Different Velocities

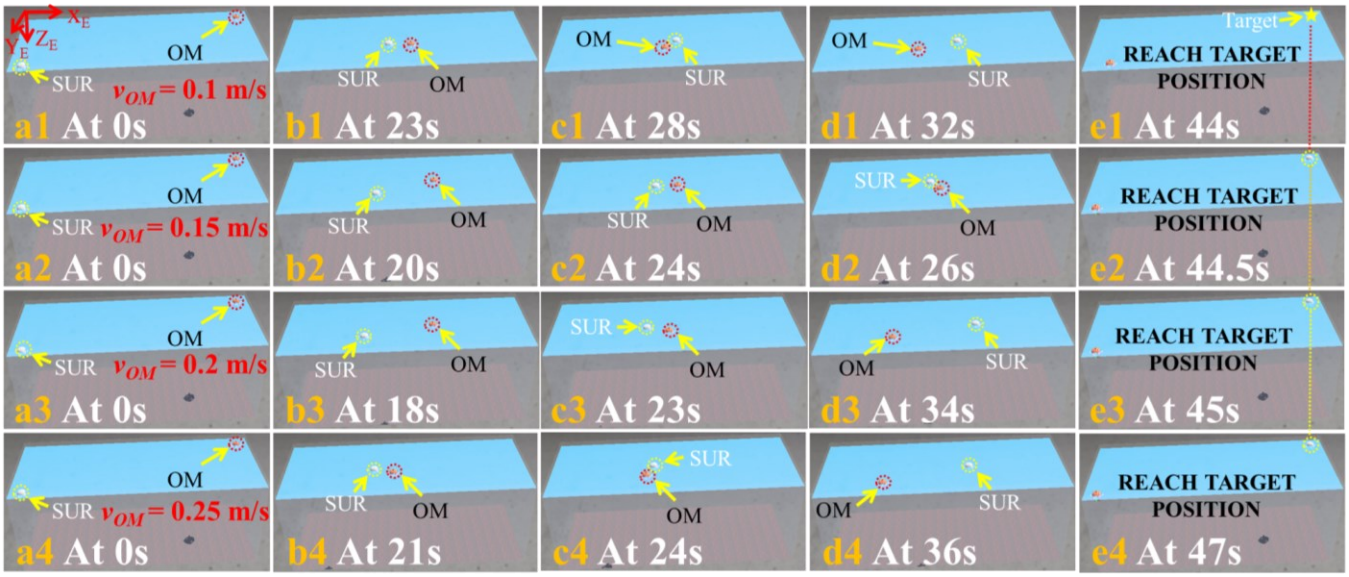

Fig. 16. Following process of SUR under moving obstacle with different velocities (in simulation).

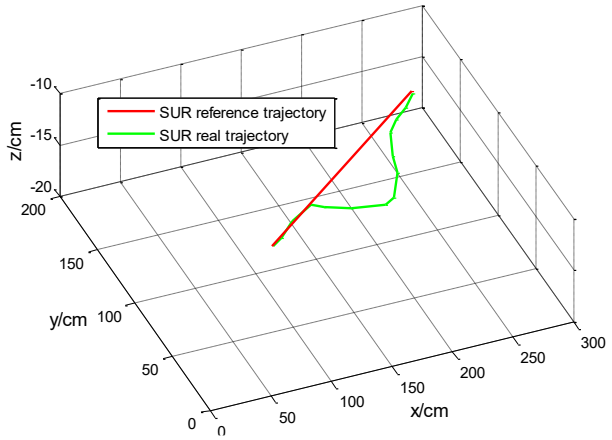

Fig. 15. Trajectory tracking result of SUR in presence of the moving obstacle behind.

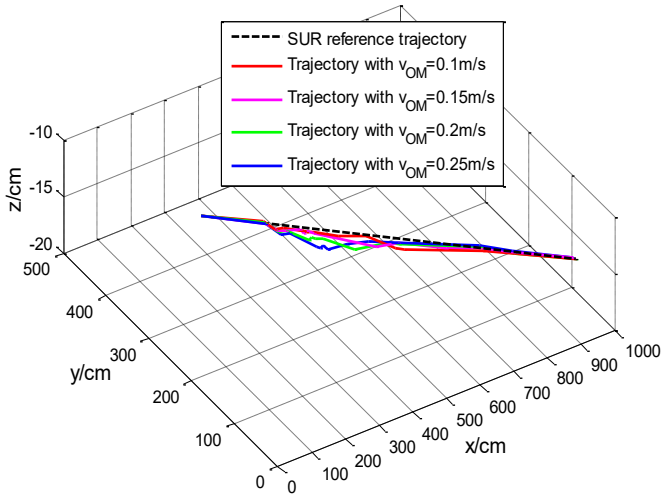

Fig. 17. Trajectory tracking result of SUR under moving obstacle with different velocities (in simulation).

After completing the avoidance experiment under moving obstacles, the obstacle velocity is considered to verify the effectiveness and flexibility of the proposed control strategy for Fig. 16. The starting and target positions were the same for each set of experiments. Since the average velocity of the SUR robot is about 0.15m/s, the velocities 0.1 m/s, 0.15 m/s, 0.2 m/s and 0.25 m/s are selected respectively.

The trajectory tracking results of SUR are shown in Fig. 17. It can be seen that SUR can safely avoid the moving obstacle (*OM*) until reaching the target position. It can be clearly seen that with the velocity of the moving obstacle, the position to avoid the obstacle is different, but the overall trending of the obstacle avoidance is the same. It also can be seen from the X/Y and Z coordinate curves that when no obstacle is detected, the curve of the robot motion is nearly the same.

It can be seen from Fig. 16 that when the velocity of the moving obstacle (*OM*) is about 0.15m/s, the time for SUR to reach the target position is about 44.5 s. When the velocity of the moving obstacle is less than 0.2 m/s, the SUR reaches the target position in less than 45 s. It is worth noting that when the velocity of the moving obstacle is 0.25 m/s, the time to reach the target position is greater than 45 s, about 47 s, which is because in the simulation, the maximum moving velocity of the SUR is set to 0.22 m/s. Secondly, when the velocity of the moving obstacle is greater than 0.22 m/s, namely $v_{OM} > 0.22$ *m/s*, the time of obstacle avoidance will also increase (related to the deflection angle of the SUR) to avoid collision with the obstacle (see Fig. 17 (blue curve)).

In addition, the experiment in the real environment was performed by changing the velocity of the moving obstacle. In order to analyze the influence of the moving obstacle velocity on the overall performance, the velocity as 0.1 m/s, 0.15 m/s, 0.2 m/s, and 0.25 m/s were selected respectively, which is the same value as in the simulation.

Fig. 18 shows the obstacle avoidance process when the velocity is 0.1 m/s and 0.15 m/s. The settings are as follows: the starting and target positions of the SUR are *(0.25 m, 1.0 m)* and *(2.75 m, 1.0 m)*, respectively. The Moving Obstacle starts from the target position *(2.75 m, 1.0 m)* and moves along a straight line. Fig. 19 shows the trajectory tracking results. From the perspective of time, when the velocity is less than 0.2 m/s, the

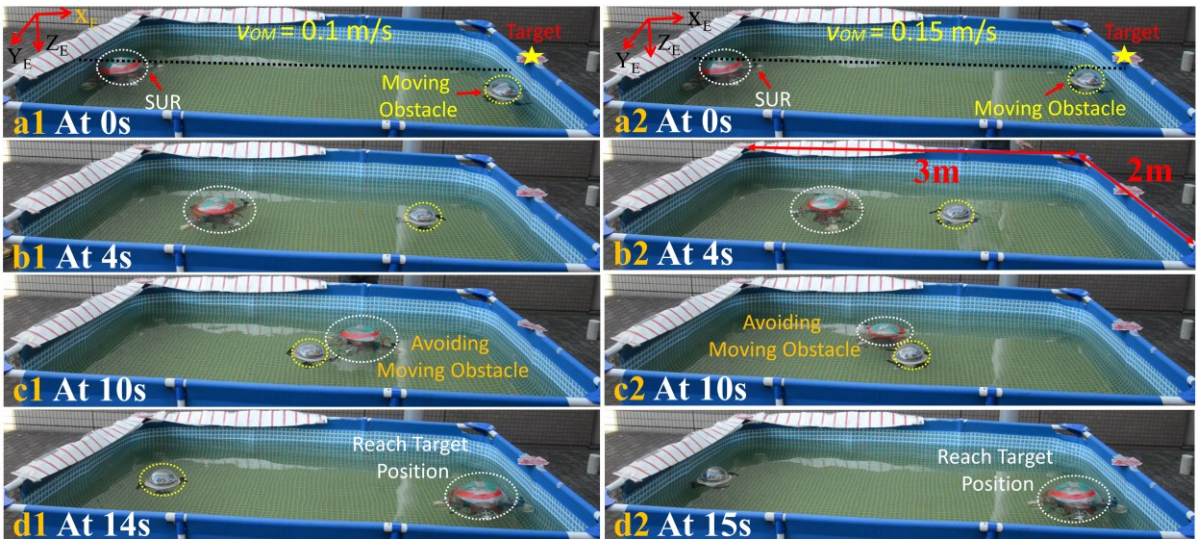

Fig. 18. Following process of SUR under moving obstacle with different velocities (in real environment).

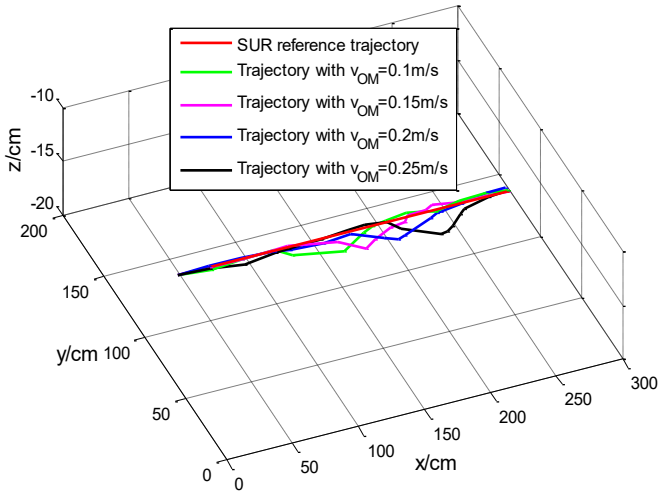

Fig. 19. Tracking result of SUR under moving obstacle with different velocities (in real environment).

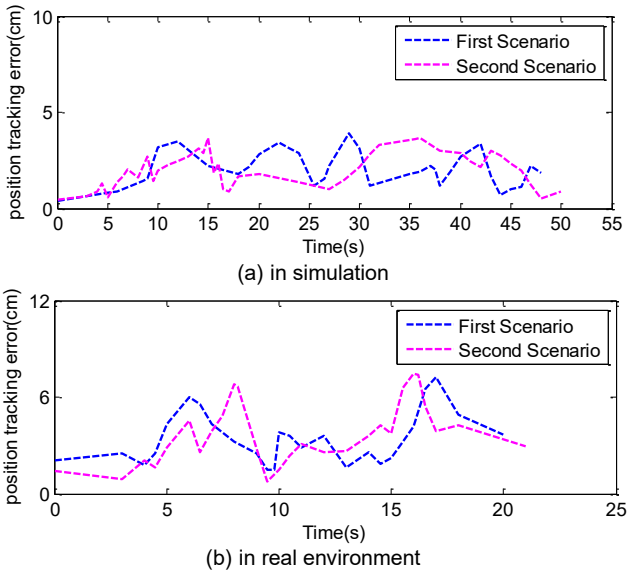

Fig. 20. The position tracking error in simulation and real environment.

average time for the SUR to reach the target position is less than 16 s. When the Moving Obstacle is greater than 0.2 m/s, taking 0.25 m/s as an example, the average time for SUR to reach the target position is less than 18.5 s, because the maximum moving velocity of the SUR is 0.22 m/s. Compared with the simulation experiment, the tracking error in the real environment will increase, but the SUR can safely reach the target position, and the average time difference is less than 3.5 s. The main reasons are external factors (wind, water waves), human factors (deviation caused by the initial position of the SUR), and the robot itself (such as motor heating, deflection angle, etc.).

B. Comprehensive Evaluation of the Comparative Experiments

The simulation results for the proposed control approach are presented in Figs. 5 - 8. To further verify the effectiveness of the proposed control approach, the position tracking error in three scenarios is depicted in Fig. 20 (a). From Figs. 5 - 6, the SUR first performs a cruise mission, the reference path is surrounded by four static obstacles. When the obstacles are detected, the SUR suffered the transient shock meanwhile avoiding obstacle at the $t = 8\ s$, $20\ s$, $28\ s$, $40\ s$. From Figs. 5 - 8, these figures verify the avoidance capability of the proposed control strategy for the designed multi-ultrasonic sensor array considering the static and moving obstacles. After avoiding all obstacles, the SUR can quickly follow the reference path until reaches the target position. As can be seen from Fig. 20 (a), the error profile of these scenarios with respect to the reference path, and the overall position error can be calculated by E_p, which can be written as $E_p = \sqrt{\Delta E_{px}^2 + \Delta E_{py}^2 + \Delta E_{pz}^2}$. In contrast to the position error in the real environment, see Fig. 20 (b), the simulated position error is reduced about 4 cm. The difference between the simulation results and the real environment is mainly caused by external factors, such as wind and water waves. Of course, there are other factors as well. Except the mentioned fluctuations, the experimental results are closely consistent with the simulation results, the overall error less than 8 cm with respect to the reference trajectory, which further validates that the SUR using the proposed control

strategy is more flexible and stable, and has certain practical value.

VII. Conclusions

In this paper, an obstacle avoidance strategy based on sensor array (ultrasonic sensor JSN-SR0T4) have been developed to ensure the safety of missions in presence of stationary and moving obstacles. To detect the surrounding environment with multiple independent sub-tasks, the NSB method is proposed to obtain the overall comprehensive output function, and a priority assignment model is designed based on the sensor array, the kinematic and dynamic model of SUR. Furthermore, based on the above analysis, an obstacle avoidance strategy is proposed, and the effectiveness and feasibility are validated by the Lyapunov theory. Moreover, in order to verify the effectiveness and practicability of the proposed control strategy, a series of experimental scenarios are designed, including scenarios with multiple static obstacles, and moving obstacles in front or behind. Finally, some comparative experiments are performed to evaluate the performance of the proposed control strategy. By discussing the tracking metrics, such as position error, total time and length, in simulation and experiments, the effectiveness, flexibility and practicability of the proposed control strategy are verified that the SUR can bypass obstacles successfully in an adaptive way.

References

[1] H. Xing, Y. Liu, S. Guo, L. Shi, X. Hou, W. Liu, Y. Zhao, "A Multi-Sensor Fusion Self-Localization System of a Miniature Underwater Robot in Structured and GPS-denied Environments," *IEEE Sensors Journal*, vol. 21, no. 23, pp. 27136-27146, 2021.

[2] J. Guo, C. Li, S. Guo, "Study on the autonomous multirobot collaborative control system based on spherical amphibious robots," *IEEE Systems Journal*, vol. 15, no. 4, pp. 4950-4957, 2021.

[3] Y. Wang, W. Li, S. Togo, H. Yokoi, Y. Jiang, "Survey on Main Drive Methods Used in Humanoid Robotic Upper Limbs," *Cyborg and Bionic Systems*, vol. 2021, p. 9817487, 2021.

[4] R. An, S. Guo, L. Zheng, H. Hirata, S. Gu, "Uncertain moving obstacles avoiding method in 3D arbitrary path planning for a spherical underwater robot," *Robotics and Autonomous Systems*, vol. 151, p. 104011, 2022.

[5] T. Fukuda, "Cyborg and Bionic Systems: Signposting the Future," *Cyborg and Bionic Systems*, vol. 2020, p. 1310389, 2020.

[6] X. Hou, S. Guo, L. Shi, H. Xing, H. Yin, Z. Li, M. Zhou, D. Xia, "Improved Model Predictive-Based Underwater Trajectory Tracking Control for the Biomimetic Spherical Robot under Constraints," *Applied Science*, vol. 10, no. 22, p. 8106, 2020.

[7] Z. He, L. Dong, C. Sun, J. Wang, "Asynchronous Multithreading Reinforcement-Learning-Based Path Planning and Tracking for Unmanned Underwater Vehicle," *IEEE Transactions on Systems, Man, and Cybernetics: Systems*, vol. 52, no. 5, pp. 2757-2769, 2021.

[8] X. Cao, L. Ren, C. Sun, "Research on obstacle detection and avoidance of autonomous underwater vehicle based on forward-looking sonar," *IEEE Transactions on Neural Networks and Learning Systems*, Early Access, 2022.

[9] A. Sahoo, S. Dwivedy, P. Robi, "Advancements in the field of autonomous underwater vehicle," *Ocean Engineering*, vol. 181, no. 1, pp. 145-160, 2019.

[10] J. Guo, C. Li, S. Guo, "Path optimization method for the spherical underwater robot in unknown environment," *Journal of Bionic Engineering*, vol. 17, pp. 944-958, 2020.

[11] W. Chen, Z. Liu, H. Zhang, M. Chen, Y. Zhang, "A submarine pipeline segmentation method for noisy forward-looking sonar images using global information and coarse segmentation," *Applied Ocean Research*, vol. 112, p. 102691, 2021.

[12] L. Zheng, S. Guo, Y. Piao, S. Gu, R. An, "Collaboration and task planning of turtle-inspired multiple amphibious spherical robots," *Micromachines*, vol. 11, no. 1, p. 71, 2020.

[13] J. Guo, C. Li, S. Guo, "A novel step optimal path planning algorithm for the spherical mobile robot based on fuzzy control," *IEEE Access*, vol. 8, pp. 1394-1405, 2019.

[14] R. Kobayashi, N. Kono, "Development of localization system using ultrasonic sensor for an underwater robot to survey narrow environment," *Journal of Nuclear Science and Technology*, vol. 55, no. 7, pp. 733-745, 2018.

[15] P. Yao, S. Zhao, "Three-dimensional path planning for AUV based on interfered fluid dynamical system under ocean current," *IEEE Access*, vol. 6, pp. 42904-42916, 2018.

[16] Z. Yan, M. Wang, J. Xu, "Robust adaptive sliding mode control of underactuated autonomous underwater vehicles with uncertain dynamics," *Ocean Engineering*, vol. 173, pp. 802-809, 2019.

[17] Z. Yan, J. Li, Y. Wu, G. Zhang, "A real-time path planning algorithm for AUV in unknown underwater environment based on combining PSO and waypoint guidance," *Sensors*, vol. 19, no. 1, p. 20, 2019.

[18] J. Wang, C. Wang, Y. Wei, C. Zhang, "Command filter based adaptive neural trajectory tracking control of an underactuated underwater vehicle in three- dimensional space," *Ocean Engineering*, vol. 180, pp. 175-186, 2019.

[19] T. Fossen, K. Pettersen, "On uniform semiglobal exponential stability (USGES) of proportional line-of-sight guidance laws," *Automatica*, vol. 50, pp. 2912-2917, 2014.

[20] J. Liu, M. Zhao, L. Qiao, "Adaptive barrier Lyapunov function-based obstacle avoidance control for an autonomous underwater vehicle with multiple static and moving obstacles," *Ocean Engineering*, vol. 243, p. 110303, 2022.

[21] P. Yao, Z. Xie, "Autonomous obstacle avoidance for AUV based on modified guidance vector field," *Acta Autom. Sin.*, vol. 46, no. 8, pp. 1670-1680, 2020.

[22] S. Zhang, Y. Dong, Y. Ouyang, Z. Yin, K. Peng, "Adaptive neural control for robotic manipulators with output constraints and uncertainties," *IEEE Transactions on Neural Networks and Learning Systems*, vol. 29, no. 11, pp. 5554-5564, 2018.

[23] A. Khalaji, H. Tourajizadeh, "Nonlinear Lyapunov based control of an underwater vehicle in presence of uncertainties and obstacles," *Ocean Engineering*, vol. 198, p. 106998, 2020.

[24] C. Yue, S. Guo, L. Shi, "Hydrodynamic Analysis of the Spherical Underwater Robot SUR-II," *International Journal of Advanced Robotic Systems*, vol. 10, pp. 1-12, 2013.

[25] C. Yue, S. Guo, M. Li, Y. Li, H. Hirata, H. Ishihara, "Mechatronic System and Experiments of a Spherical Underwater Robot: SUR-II," *Journal of Intelligent and Robotic Systems*, vol. 80, no, 2, pp. 325-340, 2015.

[26] Y. Li, S. Guo, Y. Wang, "Design and characteristics evaluation of a novel spherical underwater robot," *Robotics and Autonomous Systems*, vol. 94, pp. 61-74, 2017.

[27] S. Gu, S. Guo, "Performance Evaluation of a Novel Propulsion System for the Spherical Underwater Robot (SURIII)," *Applied Sciences*, vol. 7, no. 11, p. 1196, 2017.

[28] S. Gu, S. Guo, L. Zheng, "A highly stable and efficient spherical underwater robot with hybrid propulsion devices," *Autonomous Robots*, vol. 44, no. 2, pp. 759-771, 2020.

[29] C. Li, S. Guo, J. Guo, "Performance Evaluation of a Hybrid Thruster for Spherical Underwater Robots," *IEEE Transactions on Instrumentation and Measurement*, vol. 71, p. 7503110, 2022.

[30] R. An, S. Guo, Y. Yu, C. Li, T. Awa, "Task Planning and Collaboration of Jellyfish-inspired Multiple Spherical Underwater Robots," *Journal of Bionic Engineering*, vol. 19, pp. 643-656, 2022.

[31] A. Namiki, S. Yokosawa, "Origami Folding by Multifingered Hands with Motion Primitives," *Cyborg and Bionic Systems*, vol. 2021, p. 9851834, 2021.

[32] A. Ahrari, H. Lei, M. Sharif, K. Deb, X. Tan, "Design optimization of an artificial lateral line system incorporating flow and sensor uncertainties," *Engineering Optimization*, vol. 49, no. 2, pp. 328-344, 2017.

[33] G. Liu, M. Wang, L. Xu, A. Incecik, M. Sotelo, Z. Li, "A new bionic lateral line system applied to pitch motion parameters perception for autonomous underwater vehicles," *Applied Ocean Research*, vol. 99, p. 102142, 2020.

[34] B. Sahu, B. Subudhi, M. Gupta, "Stability analysis of an underactuated autonomous underwater vehicle using extended-routh's stability method," *International Journal of Automation and computing*, vol. 15, no. 3, pp. 299-309, 2018.

[35] X. Lin, S. Guo, C. Yue, J. Du, "3D Modelling of a Vectored Water Jet-based Multi-propeller Propulsion System for a Spherical Underwater

Robot," *International Journal of Advanced Robotics System*, vol. 10, p. 51537, 2013.
[36] C. Li, S. Guo, J. Guo, "Tracking Control in Presence of Obstacles and Uncertainties for Bioinspired Spherical Underwater Robots," *Journal of Bionic Engineering*, https://doi.org/10.1007/s42235-022-00268-z, 2022.
[37] H. Yin, S. Guo, M. Liu, "A Virtual Linkage-Based Dual Event-Triggered Formation Control Strategy for Multiple Amphibious Spherical Robots in Constrained Space With Limited Communication," *IEEE Sensors Journal*, vol. 22, no. 13, pp. 13395-13406, 2022.
[38] C. Yue, S. Guo, L. Shi, "Design and Performance Evaluation of a Biomimetic Microrobot for the Father-son Underwater Intervention Robotic System," *Microsystem Technologies*, vol. 22, pp. 831-840, 2016.
[39] S. Gu, L. Zhang, S. Guo, L. Zheng, R. An, T. Jiang, A. Xiong, "Communication and Cooperation for Spherical Underwater Robots by Using Acoustic Transmission," *IEEE/ASME Transactions on Mechatronics*, vol. 7, no. 11, p. 1196, 2017.
[40] A. Li, S. Guo, M. Liu, H. Yin, "Hydrodynamic Characteristics-based Adaptive Model Predictive Control for the Spherical Underwater Robot Under Ocean Current Disturbance," *Machines*, vol. 10, p. 798, 2022.

Chunying Li (Student Member, IEEE) received the M.S. degree in Control Engineering from Tianjin University of Technology, Tianjin, China, in 2020. He is currently working toward the Ph.D. degree with spherical underwater robot, Kagawa University, Japan. He has authored or coauthored more than 17 refereed journal and conference papers. His research interests include underwater robot, control algorithm, path tracking, sensor array and underwater cooperation.

Shuxiang Guo (Fellow, IEEE) received the Ph.D. degree in mechano-informatics and systems from Nagoya University, Nagoya, Japan, in 1995.

He is currently a Chair Professor with the Key Laboratory of Convergence Medical Engineering System and Healthcare Technology, Beijing Institute of Technology, Beijing, China. His current research includes biomimetic underwater robots, minimal invasive surgery robot systems, and rehabilitation robotics.

Dr. Guo is an Editor-in-Chief of the *International Journal of Mechatronics and Automation*.

Jian Guo received the M.S. and Ph.D. degrees in intelligent machine system from Kagawa University, Japan, in 2009 and in 2012, respectively.

Dr. Guo is currently a Professor at Tianjin University of Technology, Tianjin, China. He has published about 50 refereed journal and conference papers in recent 3 years. His research interests include biomedical robot, and underwater robot.